EN ROUTE TO VISUALIZATION OF PATHOLOGICAL EVENTS ASSOCIATED WITH CYSTIC FIBROSIS: DEVELOPMENT OF FLUORESCENT PROBES FOR MONITORING VISCOSITY OF MUCUS

by

David Edwards

Submitted in partial fulfillment of the

requirements for Departmental Honors in

the Department of Chemistry and Biochemistry

Texas Christian University

Fort Worth, Texas

May 4, 2020

EN ROUTE TO VISUALIZATION OF PATHOLOGICAL EVENTS ASSOCIATED WITH CYSTIC FIBROSIS: DEVELOPMENT OF FLUORESCENT PROBES FOR MONITORING VISCOSITY OF MUCUS

Project Approved:

Supervising Professor: Sergei Dzyuba, Ph.D.

Department of Chemistry and Biochemistry

Eric Simanek, Ph.D.

Department of Chemistry and Biochemistry

Giridhar Akkaraju, Ph.D.

Department of Biology

ABSTRACT

Boron-dipyrromethene dyes, commonly known as BODIPY dyes, are fluorescent molecules whose photophysical properties could be fine-tuned by relatively straightforward synthetic manipulations.[1] While the scaffold of the dye remains the same, substituents can be added to the BODIPY dye to produce a diverse range of BODIPY dyes. Arguably, this is one of the biggest advantages that BODIPY dyes have over other types of fluorescent dyes. Furthermore, BODIPY dyes are chemically inert, which allows their applications in various types of media, including biologically-relevant ones. Since photophysical properties of BODIPY dyes are impacted by properties of the environment (e.g., viscosity, polarity, pH, etc), there is a possibility to utilize BODIPY dyes to function as environment-sensitive small molecular probes.

While these dyes have a wide variety of applications, our group has specifically considered their use in the study of cystic fibrosis. The viscosity of the mucus secreted from mucin granules is being explored due to its relationship to the pathology of cystic fibrosis. Cells affected by cystic fibrosis demonstrated elevated levels of mucus viscosity within their mucin granules. Early detection of the elevated viscosity levels could be beneficial in starting treatment in the early stages of the disease.

1. INTRODUCTION

1.1. Importance of BODIPY dyes

Viscosity is one of the fundamental properties of fluids. Importantly, viscosity modulates the diffusion rates as well as intermolecular interaction of various species.[2] In regard to biologically relevant environments, it is known that changes of cellular viscosity, for example, could be linked to various types of pathology.[2] Thus, studies directed towards evaluation and monitoring of the viscosity are important from both fundamental and applied points of views. Molecular viscometers are among the most promising and versatile tools for assessing viscosity of biological systems. These synthetic small molecules are typically based on fluorogenic dyes, in view of high sensitivity of fluorescence (Figure 1). Fluorescence is a non-invasive and non-destructive process that is a preferred technique to track changes and events in cellular

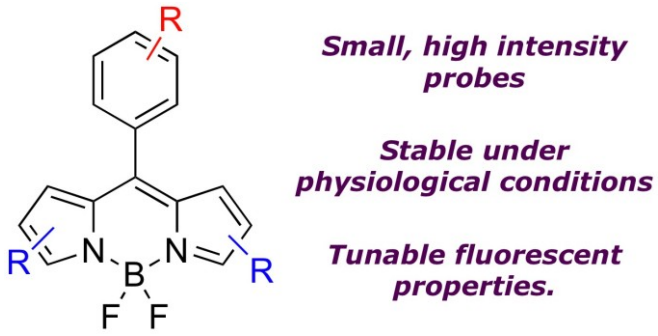

Figure 1. General structure of BODIPY dyes. R and R groups are various functionally and structurally diverse substituents.

environments. Fluorescence is a useful method due to low auto-fluorescence of the biological systems, which significantly reduces background interference and increases the sensitivity of detection.

On the molecular level, the mechanism of viscosity sensing by molecular probes, including BODIPY-based probes, is fairly complex, as it relates to the conformational changes associated with intramolecular rotations of various moieties of the probe's scaffold in the excited states (Figure 2).[3] The molecular viscometers could also be referred to as molecular rotors due to these internal rotations. In general, the intramolecular rotations produce different molecular conformations, which in turn possess different photophysical properties, such as fluorescence lifetimes, intensities, quantum yields, etc. Different viscosities of the media will have a unique impact on fluorescence lifetimes, as the intramolecular rotation of the dye will vary based on the medium. As a result, the viscosity of the medium can be quantified through measurement of the fluorescent lifetimes of the BODIPY probes that are placed within that medium.[4]

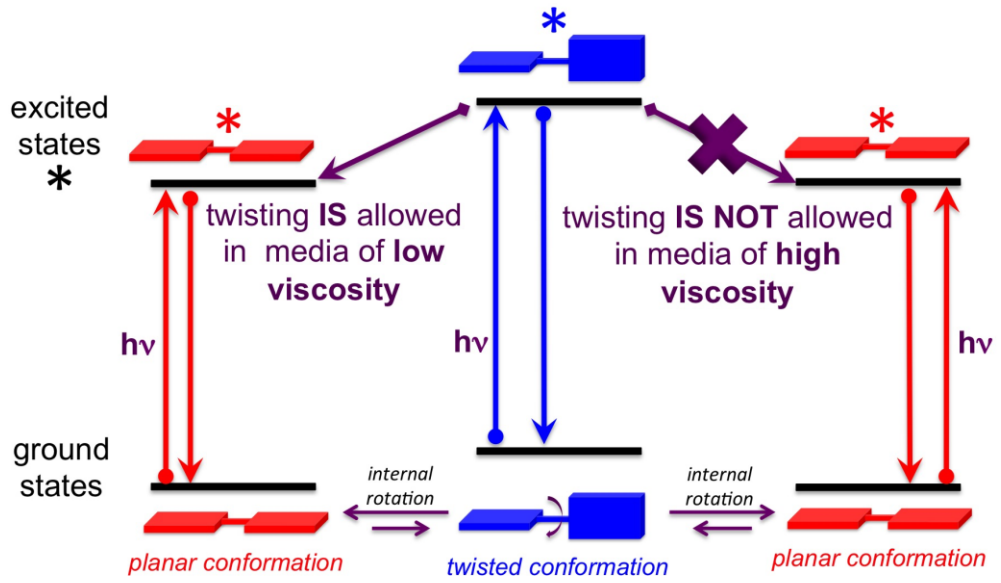

Figure 2. A general, simplified diagram of viscosity sensing by a molecular rotor that utilize intramolecular rotation between twisted (blue) and planar (red) conformations of the rotor upon light excitation (hν).

In regard to BODIPY-based molecular viscometers, there are two main classes that could be identified (Figure 3): rotors (these function as molecular viscometers, and the internal rotation is sensitive to variations of the viscosity of the media) and non-rotors, where the internal rotation is inhibited due to structural modifications (these probes function as controls to assure that the variations of photophysical properties of the probes are related strictly to viscosity variations of the media, rather than polarity, pH, or other parameters). Furthermore, non-rotor BODIPY dyes must be isomeric to rotor BODIPY dyes to assure that they have solubility profiles that are similar to rotors' congeners.

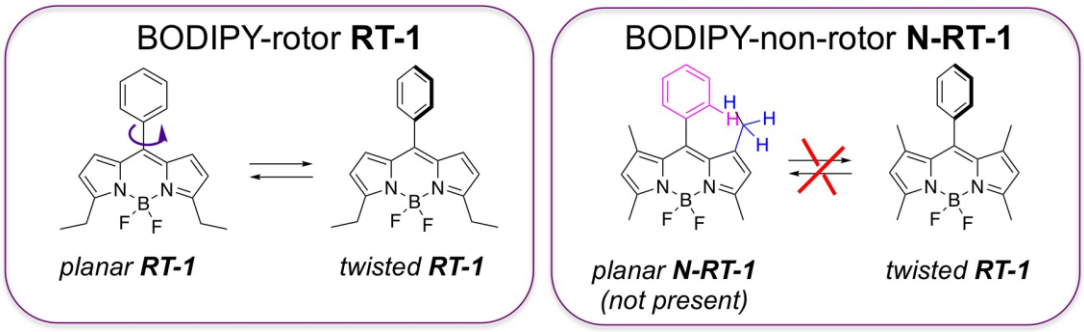

Figure 3. Internal rotation between phenyl group and BODIPY-scaffold producing planar and twisted conformations of the dyes **RT-1** (left) and **N-RT-1** (right). The planar conformation of **N-RT-1** is not attainable due to the steric interference between the H of the phenyl group (pink) and methyl-group of BODIPY (blue).

Over the past several years, the Dzyuba research group has focused on the development of BODIPY dyes that sense fluctuations of viscosity of various types of media.[5] Several molecular viscometers/rotors based on BODIPY-scaffolds have been developed. The primary

goal, from the synthetic point of view, is to design and synthesize dyes using facile, robust, and modular approaches. An optimal synthetic design should allow access to both rotors and non-rotors, and utilize as few chemical transformations as possible.[5]

1.2. Syntheses of BODIPY dyes

BODIPY dyes are typically prepared via multicomponent, solution-based syntheses.[1] These syntheses are typically characterized by long reaction times, purifications that involve chromatography, and moderate to low yields (Scheme 1).[1] Despite the fact that chromatography is one of the best and most widely used techniques to obtain pure materials, the amount of generated waste (in regard to sorbent and organic solvents) suggests that other approaches, such as extraction and crystallization (which produce lesser amounts of waste, and are more applicable for large scale syntheses), should be explored. Our group developed a more facile, almost solvent-free mechanochemical approach, which reduced reaction times

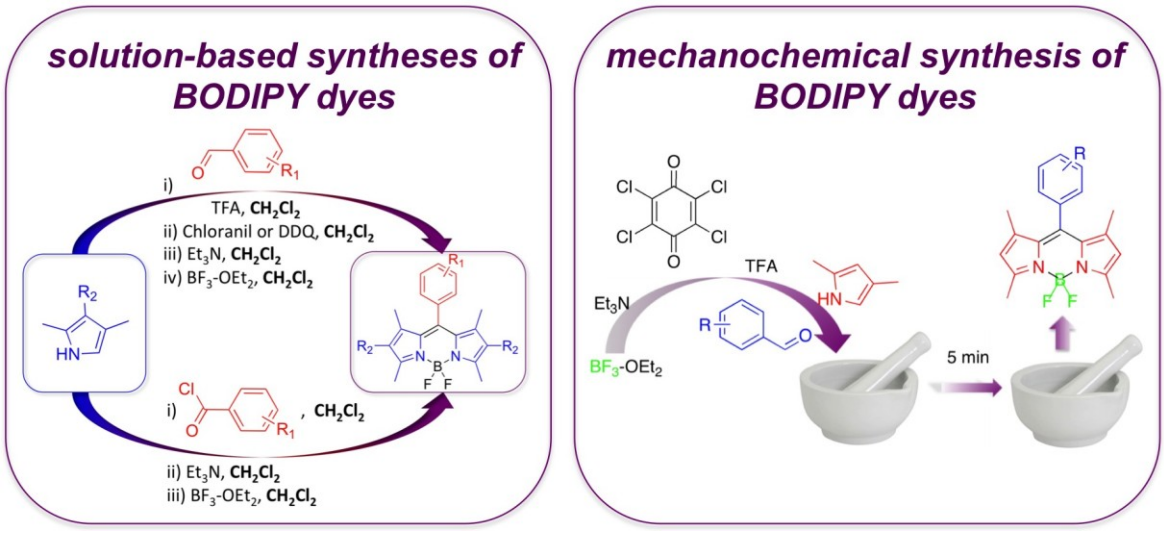

Scheme 1. Conventional, solution-based (left) and mechanochemical (right) synthesis of BODIPY dyes.

from days to minutes (Scheme 1).[5,6] However, the efficiency of the process as well as the need for chromatographic purification of the dyes, indicates that further optimizations are still required. Over the course of this project, continuous attempts were made to identify more efficient and facile modifications that would allow circumventing the need for chromatographic purification.

1.3. General considerations on cystic fibrosis

Cystic fibrosis is an autosomal recessive genetic disorder that primarily affects the function of respiratory and digestive systems, primarily due abnormal accumulation of mucus.[7] Cystic fibrosis is the result of a mutation in the gene that controls the cystic fibrosis transmembrane conductance regulator (CFTR) found in epithelial cells throughout the body. While CFTR exists in a variety of organs, it is most commonly known for its effect on the respiratory system. The CFTR is responsible for regulating cellular anion transport and for controlling removal of mucus from the respiratory system. When the function of the CFTR becomes compromised, mucus (whose primary physiological role is to protect organs from exposure to various toxins and particulates) accumulates in the lungs, leading to infection and inflammation. The malfunction of CFTR occurs primarily in epithelial cells, yet can create problems in a variety of organs ranging from the liver to the skin.[7]

In regards to pulmonary function, cystic fibrosis creates respiratory infection by dehydrating the mucus within the epithelial cells of the lungs. This mucus becomes viscous, thick, and sticky, making it hard to clear from the lungs. Under normal conditions, mucus in the lungs traps inhaled bacteria and particles. This mucus is then excreted from the respiratory

system *via* the mucociliary transport system. The mucociliary transport system utilizes cilia lining the epithelium of the airways to move mucus out of the lungs. Under conditions produced by cystic fibrosis, the mucus becomes trapped in the lungs of afflicted patients. This mucus harbors pathogens that remain in the lungs rather than being cleared out. The inability to clear mucus eventually leads to infection. In addition to the increased pathogen concentration in the lungs, cystic fibrosis patients experience inflammation up to ten times greater than a patient without cystic fibrosis with the same quantity of pathogen population. This excessive inflammatory response adds further damage to sensitive pulmonary tissue.[7]

Cystic fibrosis can drastically impair respiration and ultimately lead to premature death of those afflicted with the disease.[7] This disorder has been extensively researched over the last several decades, leading to significant increases in quality and longevity of life in patients afflicted with cystic fibrosis. However, to this date, there is no cure for cystic fibrosis, and patients inevitably succumb to respiratory failure as a result of the disease.

1.4. Importance of physical properties of mucus and their relationship to the pathology

The viscosity of the mucus secreted from mucin granules is being explored due to its potential relationship to the progress of cystic fibrosis.[8] The viscosity of mucus within mucin granules of epithelial cells within the respiratory system is elevated in individuals with cystic fibrosis. Early detection of elevated mucus levels within these granules might be useful in the development of potential remedies.

Currently there are several techniques to measure the viscosity of mucus, which can be divided into macrorheological and microrheological techniques.[8] Macrorheological techniques,

such as plate-rheometry, are capable of measuring mucus viscosity. However, they typically require significant volumes (on the order of hundreds of microliters, μL) of mucus. Obtaining these large quantities of mucus can be a significant limitation to mucus viscosity testing. Microrheological techniques, such as magnetic microrheometry, require significantly lower quantities of mucus (usually as little as 2-5 μL) to determine its viscosity. Still, this technique has limitations, such as risk of mucus dehydration due to the small volumes being tested at a time, which might compromise the integrity of the sample, and thus lead to erroneous results. Furthermore, magnetic microrheometry is limited in its ability to measure rheological properties of mucus with high viscosity only. Importantly, the aforementioned techniques do not provide non-invasive, real-time monitoring of mucus viscosity, since the mucin granules must be broken to get mucus. Arguably, this process might be compromising rheological properties, thus making it impossible to access the true parameters that might be responsible for the pathological outcomes.

Recently, our group, as a part of an international collaborative team, demonstrated that BODIPY dyes that could be used to measure intragranular mucin viscosity (Figure 4).[9] Remarkably, these simple probes dyes possessed sufficient membrane permeability which lead to their accumulation within mucin granules. In addition, small amounts of dyes were sufficient to obtain detectable signals, which assured that no perturbation of the cellular and/or membrane type of environments would be taking place.

The results of this study demonstrated that viscosity in cystic fibrosis granules is heterogeneous, as two distinct populations had been identified.[9] This is in contrast to fairly uniform, homogenous population of viscosities were observed in healthy cells (Figure 4). The

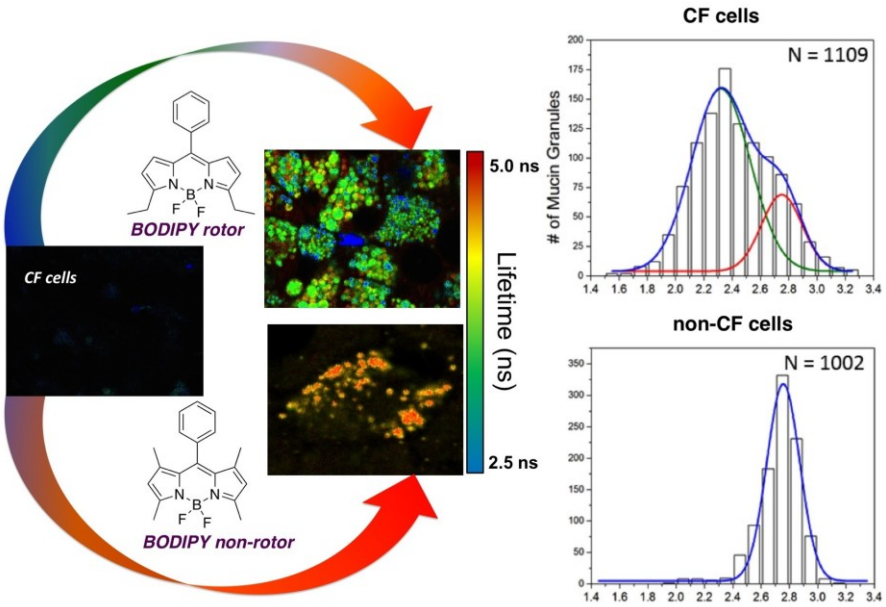

Figure 4. **RT-1** as a molecular viscometer for monitoring mucin viscosity in cystic fibrosis (CF) and non-cystic fibrosis (non-CF) cell. **N-RT-1** was used as a control.

potential of BODIPY-based viscometers for evaluating rheological properties of intact granules in live cells was demonstrated. It is plausible that synergism between synthetic molecular viscometers with fluorescent-based techniques will advance the knowledge about the effect of mucin's viscosity on various stages of cystic fibrosis.

2. RESULTS AND DISCUSSION

2.1. Synthesis of novel BODIPY-rotors and BODIPY-non-rotors as potential viscometers for assessing mucin's viscosity

Based on the published account that established the ability of a simple BODIPY rotor to measure viscosity variations within mucin granules (Figure 4), we decided to prepare a small

library of BODIPY-rotors and BODIPY-non-rotors using a general protocol developed in the Dzyuba laboratory[6] (Scheme 2). The goal was to introduce structurally and electronically diverse substituents into the aromatic substituent in the *meso*-substituent of the BODIPY scaffold, without altering the synthetic scheme. Functionalities such as alkyne, hydroxyl, alkyl, and other were successfully incorporated, and provided some degree of variation to assess the effect of electron-donating/withdrawing abilities, hydrophobic/hydrophilic properties, and H-bonding on monitoring mucin's viscosity. Although the yields of the rotors and non-rotors were moderate to poor, we made a decision not to optimize the procedures at this point, since even these low yields provided sufficient amounts the dyes for the subsequent spectroscopic, biological and rheological evaluations.

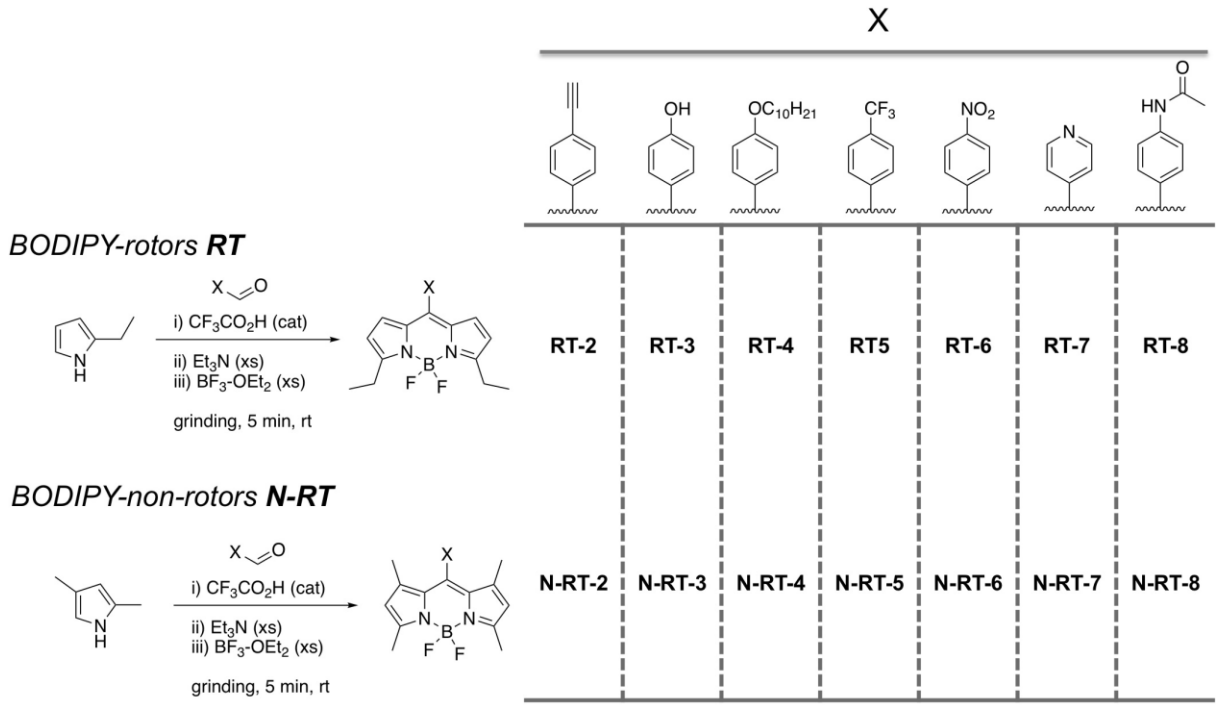

Scheme 2. Mechanochemical synthesis of BODIPY-rotors/**RT**s and BODIPY-non-rotors/**N-RT**s.

2.2. Cell penetration study by BODIPY-rotors

In order to establish the scope of BODIPY-based rotors that could be used as molecular viscometers for assessing viscosity of mucin, the uptake by Calu-3 cells of BODIPY-rotors (i.e., **RT-1** and other RTs shown in Scheme 2) was evaluated by the group of Professor Grygorczyk at the University of Montreal (Figure 5). These preliminary results indicated that incorporation of a substituent on the aromatic-group in the *meso*-position of the BODIPY rotors decreases the cell permeability of the dyes, as compared to the unsubstituted BODIPY-rotor **RT-1**. Notably, the BODIPY rotors could be broken down into three distinct groups: 1) the BODIPY-rotor **RT-1** has a very fast uptake; 2) BOIDPY rotors **RT-2**, **RT-5**, **RT-6** and **RT-8** that show a steady, gradual uptake was noted; 3) BODIPY-rotors **RT-3**, **RT-4** and **RT-7** that showed the least efficient uptake rate. It could be argued that the speed of uptake might not be absolutely crucial, as long the

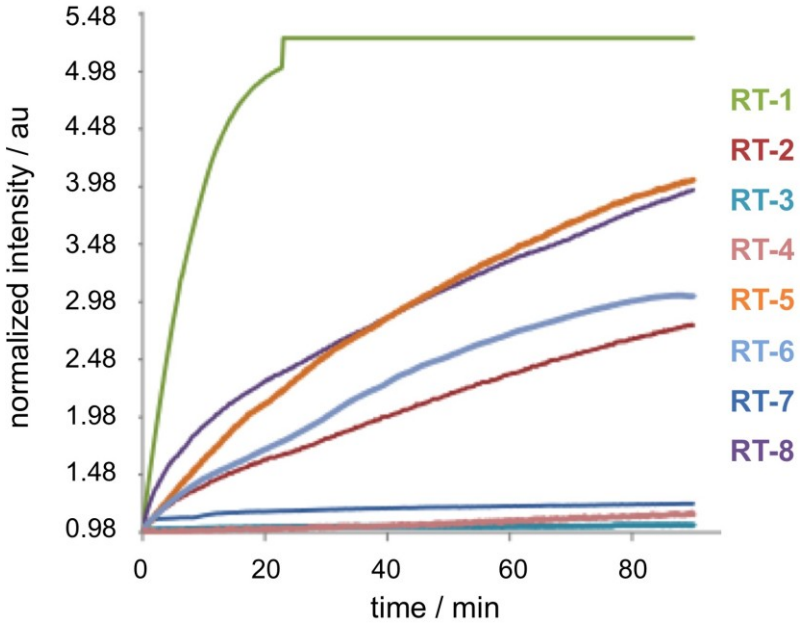

Figure 5. Kinetics of cell permeability of BODIPY-rotors.

dyes can penetrate the cell. Therefore, the dyes in "group-2", *i.e*., **RT-2**, **RT-5**, **RT-6** and **RT-8** would still be

valuable for future studies. These dyes also illustrate that modification of the *meso*-substituted position on the BODIPY scaffold is tolerated. The use of BODIPY dyes as molecular viscometers for accessing rheological properties of mucin is still ongoing in the laboratory of Professor Grygorczyk.

2.3. Synthesis of pH-sensitive BODIPY-rotors

Viscosity of mucin as well as that of mucus could be impacted by media parameters such as pH and polarity.[8-10] Therefore, it would be valuable to have molecular environment-sensitive probes that could report on those parameters as well, in addition to measuring viscosity. In principle, two distinct probes could be used, *i.e*., a molecular viscometer and a pH-sensor. However, a more appealing proposition would be to use a single probe that would be responsive to both pH and viscosity variations.

We decided to explore the possibility of introducing pH-sensitive groups onto the BODIPY-rotor and BODIPY-non-rotor scaffolds. It should be pointed out that dyes **RT-7** and **N-RT-7** (Scheme 2) have a pyridine moiety that could act as a pH-responsive unit (even though cell permeability profile was among the worst of the tested rotors). However, it is expected that due to a relatively high basicity of pyridine, the pH response window of both **RT-7** and **N-RT-7** will be fairly narrow. Thus, we considered other groups to be introduced onto the BODIPY-scaffold. Specifically, N,N-dimethylamino-containing BODIPY dyes (**RT-9** and **N-RT-9**) were prepared (Scheme 3) by utilizing the same general procedure for other BODIPY dyes (Scheme

2). These dyes should respond within a different pH-window as compared to **RT-7** and **N-RT-7** due to different basicity of dimethylamino-group as compared to pyridine.

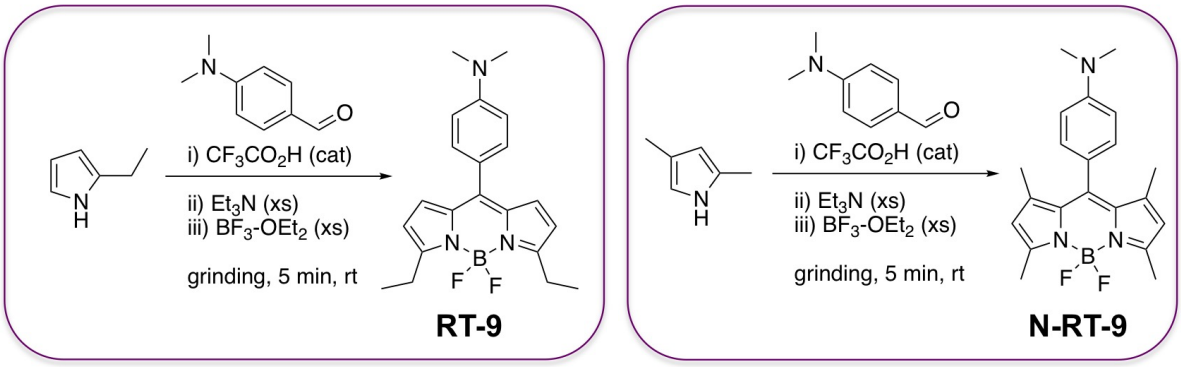

Scheme 3. Mechanochemical synthesis of dimethylamine-containing BODIPY rotor (left) and BODIPY-non-rotor (right) dyes.

In addition, NO_2-containing BODIPY dyes, **RT-6/N-RT-6**, were reduced to NH_2-containing BODIPY dyes, **RT-10/N-RT-10** (Scheme 4). These amine-containing dyes could not only be used

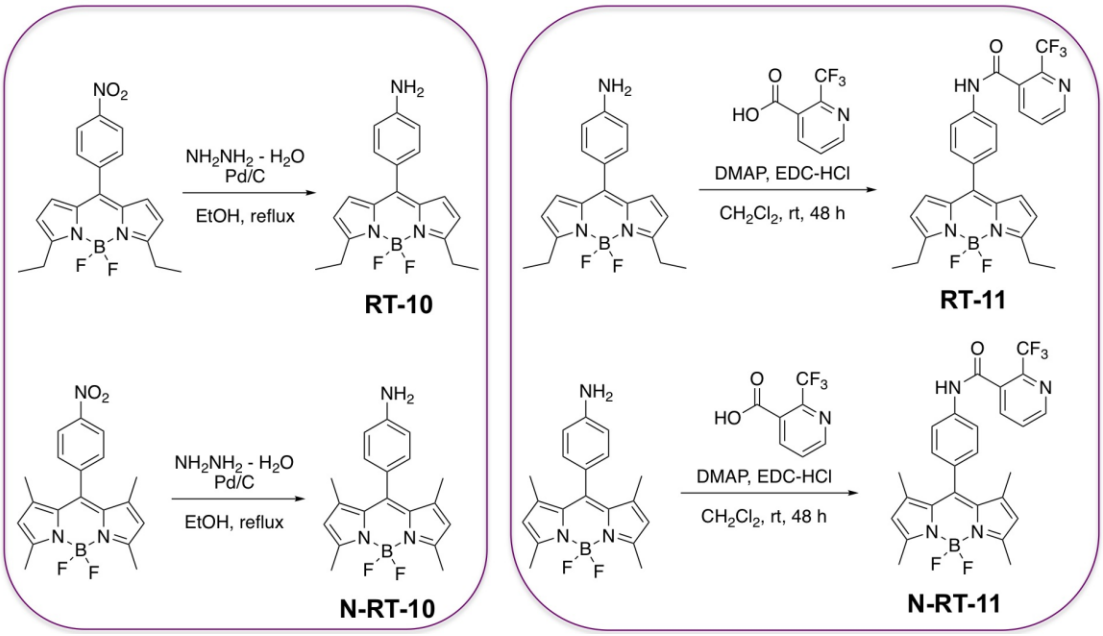

Scheme 4. Synthesis of amino-containing (left) and trifluomethylpyridine-containing (right) BODIPY rotors and non-rotors.

for pH-sensing, but also they could be used as a starting platform for incorporation of other pH-sensing groups. For example, amidation of **RT-10/N-RT-10** was explored as a method to introduce trifluomethyl-pyridine-containing groups (Scheme 4). It is anticipated that the trifluoromethyl-group in dyes **RT-11/N-RT-11** would modulate the pH response window as compared to **RT-7**/**N-RT-7**.

The spectroscopic profiles of BODIPY dyes **RT-7**/**N-RT-7**, **RT-9/N-RT-9**, **RT-10/N-RT-10** and **RT-11/N-RT-11** as a function of media's pH will be conducted in due course by the members of the Dzyuba research group, and more detailed investigations will be done in collaboration with the group of Professor Gryczynski (TCU/Department of Physics and Astronomy).

2.4. Initial trials for non-chromatographic purification of BODIPY dyes

During our synthetic studies on the synthesis of BODIPY-rotors and BODIPY-non-rotors, we found that the yields of dye ranged from poor to moderate. In principle, low yields could be explained by the one-pot multicomponent nature of the synthesis, that involves multiple elaborate mechanistic steps. In addition, chromatographic purification of the desired compounds appeared to be challenging. In all instances, after column chromatography, the sorbent (SiO_2 or Al_2O_3) appeared to retain substantial amounts of fluorescent material. Any attempts to remove this fluorescence material proved to be inefficient (*i.e.*, large amounts of various solvents were required, additional chromatographic purification was required). Therefore, we attempted to develop a chromatography-free purification procedure. Towards this end, we decided to use a symmetric BODIPY dye **12** as a model synthesis (Scheme 5). The

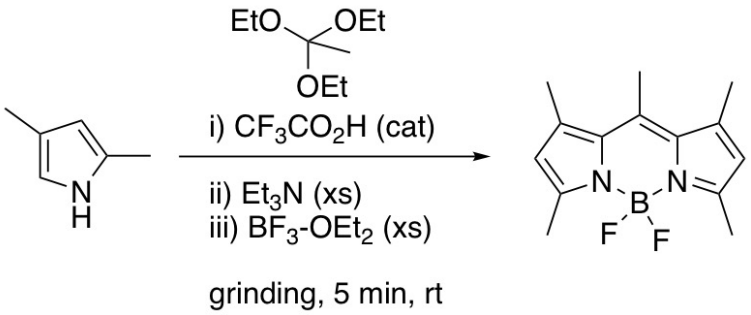

Scheme 5. Mechanochemical synthesis of symmetric BODIPY dye **12**.

compound was purified using column chromatography (see *Procedure A*, in section 3.3). It should be noted that recrystallization of the crude reaction mixture was tried using a number of organic solvents and mixtures of organic solvents. However, all these crystallization attempts proved inefficient as either the crystalline product could not be obtained or insignificant amounts of only a relatively pure **12** were obtained (*ca.* 80 % purity as established by ^{1}H NMR spectrometry). As a result, crystallization as a purification protocol was abandoned.

Next, we focused on exploring liquid-solid extraction to purify crude **12**. Due to partial solubility of **12** in diethyl ether and petroleum ether, the crude **12** was subjected to extraction with these solvents (see *Procedure B*, in section 3.3). The rationale for this approach was based on the fact that **12** possessed higher solubility in ethers than the impurities. The TLC analysis of the Et_2O fractions indicated the presence of impurities (*i.e.*, in addition to the fluorescent spot, other UV-active spots were noted). The amount of extracted dye was low even after 4 extraction cycles. Furthermore, the presence of appreciable amounts of dye **12** in the solid was also noted, albeit along with significant amount of other UV-active species. To decrease solubility of **12**, Et_2O was substituted with petroleum ether. However, all attempts to obtain a

TLC-pure dye in any appreciable quantity failed. As a result, liquid-solid extraction methods using ethers was abandoned.

As an alternative strategy, we decided to capitalize on the fact that **12** was not soluble in water, yet some impurities appeared to have some solubility in water (as was evident by colorization of aqueous layers during the extraction steps). To our surprise, subjecting crude **12** to liquid-solid extraction procedure using water (see *Procedure C*, in section 3.3) gave TLC- and NMR-pure dye in appreciable quantity, which surpassed that obtained using column chromatography (which is considered to be the most efficient method for BODIPY dyes' purification). Despite this successful result, it should be kept in mind that it is quite preliminary and further studies with a wider scope of the dyes will be required to suggest this as a general purification method for BODIPY dyes.

3. EXPERIMENTAL PART

3.1. Materials and methods

All reagents and solvents were purchased from the commercial courses (Sigma-Aldrich, Acros, and TCI) and were used as received. 4-(Decyloxy)benzaldehyde was prepared by Guillaume Douady. Column chromatography was performed using silica gel (Silicycle) or basic alumina (Brockman I, Sigma-Aldrich). Fractions were monitored by TLC (silica gel 60 F254), and the spots were visualized using UV-vis lamp (equipped with short/long wavelengths settings). NMR spectra were acquired on Bruker (400 MHz) spectrophotometer, and the chemical shifts

are reported in ppm (δ) from tetramethylsilane or residual solvent peak. Multiplicities are reported as: s – singlet, d – doublet, t – triplet, m – multiplet.

3.2. General synthetic procedures, and NMR characterization of BODIPY-rotors and BODIPY-non-rotors

BODIPY dyes 2-8 (both rotors/**RT** and non-rotors/**N-RT**) were prepared according to published procedure[6] typically on a 1-gram scale (based on pyrrole). In a well-ventilated hood, behind the protective shield, aldehyde (1 eq.) and pyrrole (2 eq.) were mixed briefly with a pestle in a mortar. A few drops of trifluoroacetic acid (TFA) were added *via* pipette upon mixing, and the formation of semi-solid/semi-slush mixture was noted. CH_2Cl_2 (1-2 ml) were added, and the content was grinded until a homogeneous mixture was obtained. Next, p-chloranil (1.2 eq.) was added in one portion, and grinding continued for about 30 seconds, as the formation of deep red/burgundy mixture was noted. Subsequently, Et_3N (10 eq.) was added under grinding produced a deep green mixture, which was grinded for about 1 min until homogenous paste formed. Next, BF_3-Et_2O (10 eq.) was added slowly, dropwise via syringe under continuous grinding, as the formation of deep red-metallic mixture was observed. Once the addition of BF_3-Et_2O was complete, the grinding was continued for about 1 minute till smooth, "homogeneous" paste was obtained. The resulting mixture was dissolved in CH_2Cl_2 (ca. 100 ml) and transferred into a separatory funnel, and washed sequentially with Na_2CO_3 (aq/sat) (2 x 100 ml) and brine (2 x 100 ml). Organic solvent was removed in vacuo, and the residue was subjected to column chromatography (SiO_2, $CHCl_3$ for dyes **2**-**6** and **8**; Al_2O_3/basic Brockman I, $CHCl_3$ for dye **7** and **9**) to yield the desired BODIPY dye.

BODIPY-non-rotor **N-RT-2**: Yield 34 %.

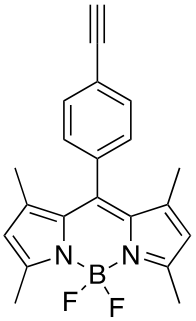

^{1}H NMR (400 MHz, $CDCl_3$): δ 7.55 (d, *J* = 8.0 Hz, 2H), 7.19 (d, *J* = 8.0 Hz, 2H), 5.91 (s, 2H), 3.11 (s, 1H), 2.48 (s, 6H), 1.32 (s, 6H). ^{19}F NMR (376 Hz, $CDCl_3$): δ –146.20 (q, *J* = 32.6 Hz).

BODIPY-rotor **RT-2**: Yield 21%.

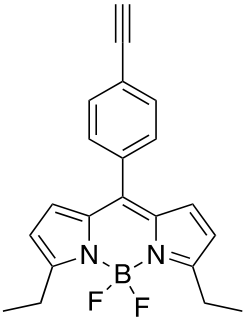

^{1}H NMR (400 MHz, $CDCl_3$): δ 7.60 (d, *J* = 8.4 Hz, 2H), 7.46 (d, *J* = 8.4 Hz, 2H), 6.72 (d, *J* = 4.0 Hz, 2H), 6.36 (d, *J* = 4.0 Hz, 2H), 3.22 (s, 1H), 3.08 (q, *J* = 7.6 Hz, 4H), 1.37 (t, *J* = 7.6 Hz, 6H). ^{19}F NMR (376 Hz, $CDCl_3$): δ –145.25 (q, *J* = 32.7 Hz). ^{11}B NMR (128 MHz, $CDCl_3$): δ 0.96 (t, *J* = 32.9 Hz).

BODIPY-non-rotor **N-RT-3**: Yield 14 %.

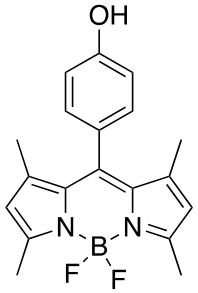

^{1}H NMR (400 MHz, $CDCl_3$): δ 7.15 (d, *J* = 8.8 Hz, 2H), 6.97 (d, *J* = 8.8 Hz, 2H), 6.00 (s, 2H), 2.57 (s, 6H), 1.47 (s, 6H). ^{19}F NMR (376 Hz, $CDCl_3$): δ –146.30 (q, *J* = 32.0 Hz). ^{11}B NMR (128 MHz, $CDCl_3$): δ 0.77 (t, *J* = 33.3 Hz).

BODIPY-rotor **RT-3**: Yield 37 %.

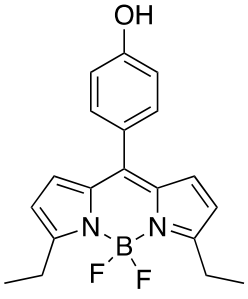

^{1}H NMR (400 MHz, $CDCl_3$): δ 7.36 (d, *J* = 8.4 Hz, 2H), 6.89 (d, *J* = 8.4 Hz, 2H), 6.76 (d, *J* = 4.0 Hz, 2H), 6.34 (d, *J* = 4.0 Hz, 2H), 3.07 (q, *J* = 7.6 Hz, 4H), 1.31 (t, *J* = 7.6 Hz, 6H). ^{19}F NMR (376 Hz, $CDCl_3$): δ –144.30 (q, *J* = 32.0 Hz). ^{11}B NMR (128 MHz, $CDCl_3$): δ 1.02 (t, *J* = 33.3 Hz).

BODIPY-non-rotor **N-RT-4**: Yield 5 %.

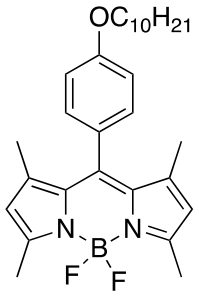

^{1}H NMR (400 MHz, $CDCl_3$): δ 7.13 (d, *J* = 8.8 Hz, 2H), 6.98 (d, *J* = 8.8 Hz, 2H), 5.97 (s, 2H), 2.54 (s, 6H), 1.81 (pent, *J* = 7.2 Hz, 2H), 1.48 (m, 2H), 1.28 (m, 14H), 1.43 (s, 6H), 0.89 (t, *J* = 6.8 Hz, 3H). ^{19}F NMR (376 Hz, $CDCl_3$): δ –145.58 (q, *J* = 32.0 Hz). ^{11}B NMR (128 MHz, $CDCl_3$): δ 0.91 (t, *J* = 33.3 Hz).

BODIPY-rotor **RT-4**: Yield 6 %.

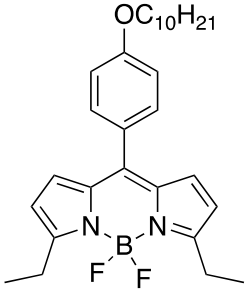

^{1}H NMR (400 MHz, $CDCl_3$): δ 7.43 (d, *J* = 8.8 Hz, 2H), 6.98 (d, *J* = 8.8 Hz, 2H), 6.79 (d, *J* = 4.4 Hz, 2H), 6.35 (d, *J* = 4.0 Hz, 2H), 4.02 (t, *J* = 6.4 Hz, 4H), 3.07 (q, *J* = 7.6 Hz, 4H), 1.83 (pent, *J* = 6.4 Hz, 2H), 1.49 (m, 2H), 1.34 (t, *J* = 7.6 Hz, 6H), 1.28 (m, 14H), 0.88 (0.89 (t, *J* = 6.8 Hz, 3H). ^{19}F NMR (376 Hz, $CDCl_3$): δ –145.22 (q, *J* = 30.1 Hz). ^{11}B NMR (128 MHz, $CDCl_3$): δ 1.01 (t, *J* = 32.0 Hz).

BODIPY-non-rotor **N-RT-5**: Yield 8 %.

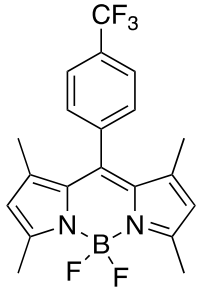

^{1}H NMR (400 MHz, $CDCl_3$): δ 7.82 (d, *J* = 8.1 Hz, 2H), 7.47 (d, *J* = 8.0 Hz, 2H), 6.04 (s, 2H), 3.84 (s, 2H) 2.59 (s, 6H), 1.39 (s, 6H). ^{19}F NMR (376 Hz, $CDCl_3$): δ – 62.51 (s, 3F), –145.93 (q, *J* = 31.9 Hz, 2F). ^{11}B NMR (128 MHz, $CDCl_3$): δ 0.78 (t, *J* = 33.3 Hz).

BODIPY-rotor **RT-5**: Yield 6 %.

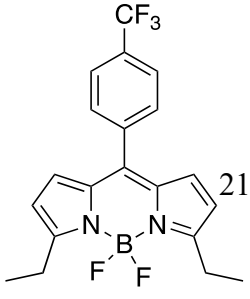

^{1}H NMR (400 MHz, $CDCl_3$): δ 7.73 (d, *J* = 8.1 Hz, 2H), 7.56 (d, *J* = 8.0 Hz, 2H), 6.63 (d, *J* = 4.0 Hz, 2H), 6.35 (d, *J* = 4.4 Hz, 2H), 3.08 (q, *J* = 7.6 Hz, 4H), 1.32 (t, *J* = 7.6 Hz, 6H). ^{19}F NMR (376 Hz, $CDCl_3$): δ –62.73 (s, 3F), –144.93 (q, *J* = 32.6 Hz, 2F). ^{11}B NMR (128 MHz, $CDCl_3$): δ 0.99 (t, *J* = 33.3 Hz).

BODIPY-non-rotor **N-RT-6**: Yield 11 %.

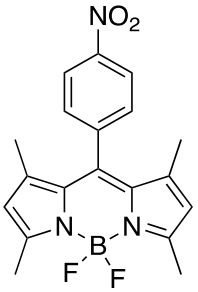

^{1}H NMR (400 MHz, $CDCl_3$): δ 8.39 (d, *J* = 8.7 Hz, 2H), 7.54 (d, *J* = 8.7 Hz, 2H), 6.02 (s, 2H), 2.57 (s, 6H), 1.37 (s, 6H). ^{19}F NMR (376 Hz, $CDCl_3$): δ –144.93 (q, *J* = 33.8 Hz).

BODIPY-rotor **RT-6**: Yield 29 %.

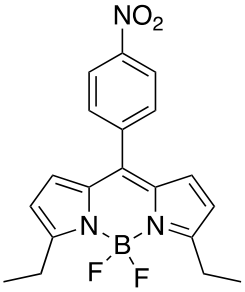

^{1}H NMR (400 MHz, $CDCl_3$): δ 8.36 (d, *J* = 8.6 Hz, 2H), 7.68 (d, *J* = 8.7 Hz, 2H), 6.65 (d, *J* = 4.1 2H), 6.39 (d, *J* = 4.1 Hz, 2H), 3.09 (q, *J* = 7.4 Hz, 4H), 1.35 (t, J = 7.5 Hz, 6H). ^{19}F NMR (376 Hz, $CDCl_3$): δ –145.26 (q, *J* = 32.4 Hz). ^{11}B NMR (128 MHz, $CDCl_3$): δ 0.94 (t, *J* = 32.4 Hz).

BODIPY-non-rotor **N-RT-7**: Yield 5 %.

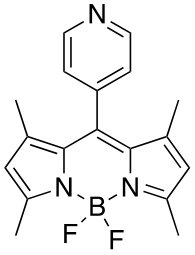

^{1}H NMR (400 MHz, $CDCl_3$): δ 8.37 (d, *J* = 6.8 Hz, 2H), 7.27 (d, *J* = 7.6 Hz, 2H), 6.05 (s, 2H), 2.56 (s, 6H), 1.58 (s, 6H). ^{19}F NMR (376 Hz, $CDCl_3$): δ –146.15 (q, *J* = 32.0 Hz). ^{11}B NMR (128 MHz, $CDCl_3$): δ 0.64 (t, *J* = 33.3 Hz).

BODIPY-rotor **RT-7**: Yield 18 %.

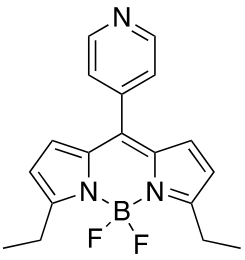

^{1}H NMR (400 MHz, $CDCl_3$): δ 8.77 (d, *J* = 5.8 Hz, 2H), 7.41 (d, *J* = 5.9 Hz, 2H), 6.68 (d, *J* = 4.2 Hz, 2H), 6.38 (d, *J* = 4.2 Hz, 2H), 3.08 (q, *J* = 7.5 Hz, 4H), 1.35 (t, *J* = 7.5 Hz, 6H). ^{19}F NMR (376 Hz, $CDCl_3$): δ –145.20 (q, *J* = 34.0 Hz).

BODIPY-non-rotor **N-RT-8**: Yield 20 %.

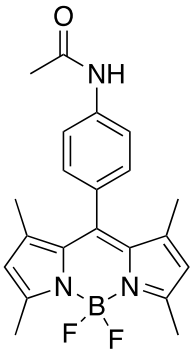

^{1}H NMR (400 MHz, $CDCl_3$): δ 7.36 (d, *J* = 8.4 Hz, 2H), 7.57 (s, 1H), 7.21 (d, *J* = 8.4 Hz, 2H), 5.98 (s, 2H), 2.55 (s, 6H), 2.21 (s, 3H), 1.41 (s, 6H). ^{19}F NMR (376 Hz, $CDCl_3$): δ –146.03 (q, *J* = 33.8 Hz). ^{11}B NMR (128 MHz, $CDCl_3$): δ 0.77 (t, *J* = 32.0 Hz).

BODIPY-rotor **RT-8**: Yield 6%.

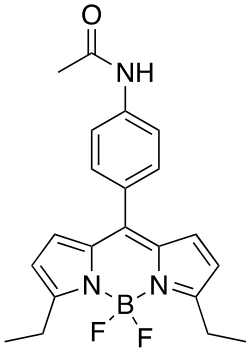

^{1}H NMR (400 MHz, $CDCl_3$): δ 7.69 (s, 1H), 7.65 (d, *J* = 8.0 Hz, 2H), 7.43 (d, *J* = 8.4 Hz, 2H), 6.74 (d, *J* = 4.0 Hz, 2H), 6.34 (d, *J* = 4.0 Hz, 2H), 3.07 (q, *J* = 7.2 Hz, 4H), 2.22 (s, 3H), 1.33 (t, *J* = 7.6 Hz, 6H). ^{19}F NMR (376 Hz, $CDCl_3$): δ –145.33 (q, *J* = 34.0 Hz). ^{11}B NMR (128 MHz, $CDCl_3$): δ 0.79 (t, *J* = 32.0 Hz).

BODIPY-non-rotor **N-RT-9**: Yield 30 %.

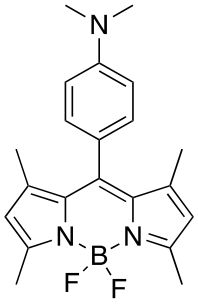

^{1}H NMR (400 MHz, $CDCl_3$): δ 7.21 (d, *J* = 7.6 Hz, 2H), 6.74 (d, *J* = 9.2 Hz, 2H), 6.18 (s, 2H), 3.13 (s, 6H) 2.91 (s, 6H), 1.41 (s, 6H). ^{19}F NMR (376 Hz, $CDCl_3$): δ –145.70 (m).

BODIPY-rotor **RT-9**: Yield 27 %.

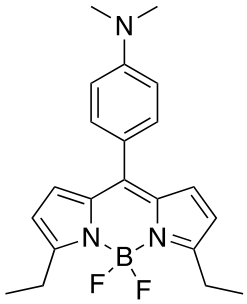

^{1}H NMR (400 MHz, $CDCl_3$): δ 7.39 (d, *J* = 8.8 Hz, 2H), 7.73 (d, *J* = 8.8 Hz, 2H), 6.62 (d, *J* = 4.0 Hz, 2H), 6.20 (d, *J* = 4.4 Hz, 2H), 3.03 (s, 6H), 2.78 (q, *J* = 7.2 Hz, 4H), 1.36 (t, *J* = 7.6 Hz, 6H). ^{19}F NMR (376 Hz, $CDCl_3$): δ –145.13 (q, *J* = 33.8 Hz).

BODIPY dyes **10** (both rotor/**RT** and non-rotor/**N-RT**) were obtained according to the following general procedure. A round bottom flask equipped with a reflux condenser was charged with a stirring bar, dye **6** (180 mg, 0.48 mmol), Pd/C (60 mg), NH_2NH_2-H_2O (0.1 ml, 2 mmol), and EtOH (2 ml). The reaction mixture was refluxed for about 4 hours, until no starting material was observed by TLC (SiO_2, $CHCl_3$). The reaction was filtered through a pad of celite, which was subsequently washed with CH_2Cl_2 (ca. 10 ml). Organic fractions were combined and the volatiles removed *in vacuo* to give the desired product, which was used for the subsequent syntheses without purification.

BODIPY-non-rotor **N-RT-10**: Yield 90 %.

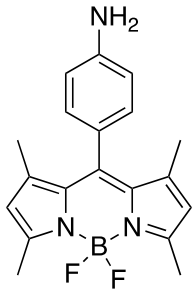

^{1}H NMR (400 MHz, $CDCl_3$): δ 7.01 (d, *J* = 8.4 Hz, 2H), 6.78 (d, *J* = 8.0 Hz, 2H), 5.97 (s, 2H), 3.84 (s, 2H) 2.54 (s, 6H), 1.41 (s, 6H). ^{19}F NMR (376 Hz,

$CDCl_3$): δ –146.32 (q, *J* = 31.9 Hz). ^{11}B NMR (128 MHz, $CDCl_3$): δ 0.78 (t, *J* = 33.3 Hz).

BODIPY-rotor **RT-10**: Yield 93 %.

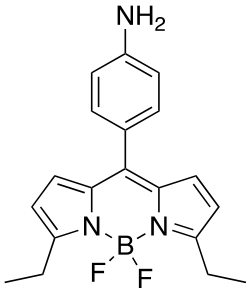

^1H NMR (400 MHz, $CDCl_3$): δ 7.18 (d, *J* = 8.8 Hz, 2H), 6.71 (d, *J* = 4.0 Hz, 2H), 6.57 (d, *J* = 8.4 Hz, 2H), 6.23 (d, *J* = 4.4 Hz, 2H), 3.91 (s, 2H), 2.98 (q, *J* = 7.6 Hz, 4H), 1.33 (t, *J* = 7.6 Hz, 6H). ^{19}F NMR (376 Hz, $CDCl_3$): δ –144.93 (q, *J* = 33.8 Hz). ^{11}B NMR (128 MHz, $CDCl_3$): δ 1.03 (t, *J* = 33.3 Hz).

BODIPY dyes **11** (both rotor/**RT** and non-rotor/**N-RT**) were obtained according to the following general procedure. A round bottom flask was charged with a stirring bar, dye **10** (50 mg, 0.15 mmol), dimethylaminopyridine/DMAP (180 mg, 0.4 mmol), N-(3-dimethylamionpropyl)-N-ethylcarbodiimide hydrochloride/EDC-HCl (38.3, 0.2 mmol), and CH_2Cl_2 (1.5 ml), and the reaction mixture was stirred at room temperature for 48 hours. Next, the volatiles were removed under vacuo, and the residue was subjected to gradient column chromatography (SiO_2, $CHCl_3$ to $CHCl_3$/ethyl acetate (4/1) to $CHCl_3$/ethyl acetate (1/1)) to give the desired dye **11**.

BODIPY-non-rotor **N-RT-11**: Yield 24 %.

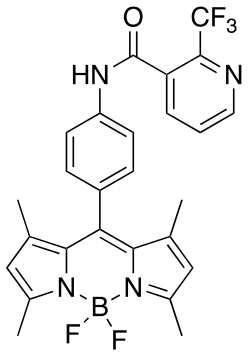

^1H NMR (400 MHz, $CDCl_3$): δ 8.85 (d, *J* = 3.6 Hz, 1H), 8.08 (d, *J* = 7.6 Hz, 1H), 8.04 (s, 1H), 7.79 (d, *J* = 8.4 Hz, 2H), 7.65 (dd, *J* = 7.6, 4.8 Hz, 1H), 7.31 (d, *J* = 8.4 Hz, 2H), 6.00 (s, 2H), 2.56 (s, 6H), 1.46 (s, 6H). ^{19}F NMR (376

Hz, $CDCl_3$): δ – 63.76 (s, 3F), –146.23 (q, *J* = 33.8 Hz, 2F).

BODIPY-rotor **RT-11**: Yield 33 %.

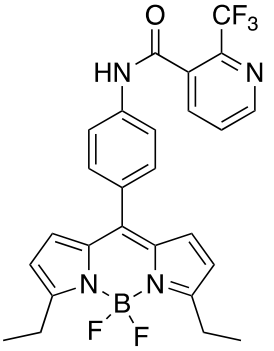

^{1}H NMR (400 MHz, $CDCl_3$): δ 8.86 (d, *J* = 4.8 Hz, 1H), 8.07 (d, *J* = 6.8 Hz, 1H), 7.73 (d, *J* = 8.8 Hz, 2H), 7.67 (m, 3H), 7.55 (d, *J* = 8.8 Hz, 2H), 6.78 (d, *J* = 4.4 Hz, 2H), 6.37 (d, *J* = 4.4 Hz, 2H), 3. 0.8 (q, *J* = 7.6 Hz, 4H), 1.35 (t, *J* = 7.6 Hz, 6H). ^{19}F NMR (376 Hz, $CDCl_3$): δ – 63.65 (s, 3F), –145.22 (q, *J* = 33.8 Hz, 2F).

3.3. Model study on the chromatography-free isolation/purification of a BODIPY dye

BODIPY dye **12** was prepared according to a modified literature procedure (BJOC 2013). In a well-ventilated hood, behind the protective shield, 2,4-dimethylpyrrole (0.5 ml, 4.91 mmol) was mixed briefly in triethyl orthoacetate (0.45 ml, 2.95 mmol) in a mortar with pestle. Next, trifluoroacetic acid/TFA (0.25 ml) was added via a pipette and the formation of a slushy solid was noted. Et_3N (4.1 ml, 29.4 mmol) was added and grinding continued for about 1 minute. Next, BF_3-Et_2O (4.1 ml, 15.1 mmol) was added slowly, dropwise, via syringe under continuous grinding. Once the addition of BF_3-Et_2O was finished, the grinding continued for about 1 minute. The residue was dissolved in CH_2Cl_2 (50 ml) and washed with 1M HCl (2 x 50ml) and brine (2 x 50 ml). Volatiles were removed in vacuo and the crude product was subjected to one of the three purification/isolation procedures outlines below.

Purification/isolation procedure A: the crude product was subjected to column chromatography (SiO_2, hexane/ethyl acetate : 4/1 v/v), and **12** was isolated in 34 % yield. ^{1}H and ^{19}F NMR analysis of the sample confirmed the identity and purity of the dye.

Purification/isolation procedure B: a round bottom flask equipped with a reflux condenser was charged with a stirring bar, crude product, and Et_2O (50 ml). The mixture was refluxed under stirring for 30 minutes. Next, the Et_2O layer was decanted, fresh Et_2O (50 ml) was added to the solid, and the mixture was refluxed under stirring for 30 minutes. This step was repeated two more times. All liquid fractions were combined and Et_2O was removed under vacuum to give **12** in 5 % yield (*ca*. 80 % purity as established by ^{1}H NMR analysis). Qualitatively similar results were obtained when petroleum ether was used instead of Et_2O.

Purification/isolation procedure C: a round bottom flask equipped with a reflux condenser was charged with stirring bar, crude product and Et_2O (100 ml). The mixture was heated (at 60-70 ^{o}C) under stirring for 30 minutes. Next, the aqueous layer was decanted, fresh water was added, and the mixture was heat (at 60-70 ^{o}C) under stirring for 30 minutes. This step was repeated two more times. The solid was filtered and dried under vacuum to give the desired dye in 47 % yield. ^{1}H and ^{19}F NMR analysis of the sample confirmed the identity and purity of the dye.

BODIPY dye **12**: ^{1}H NMR (400 MHz, $CDCl_3$): δ 6.06 (s, 2H), 2.58 (s, 3H), 2,52 (s, 6H), 2.42 (s, 6H). ^{19}F NMR (376 Hz, $CDCl_3$): δ –146.73 (q, J = 33.8 Hz).

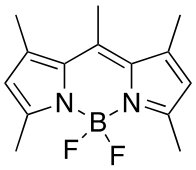

4. CONCLUSIONS

In the course of this work, various structurally and electronically diverse BODIPY-rotors and BODIPY-non-rotors were prepared in an effort to establish BODIPY dyes as molecular viscometers for assessment of rheological properties of mucin and mucus as it relates to Cystic Fibrosis. A preliminary cell permeability study indicated that several BODIPY-rotors could be used for those studies. Furthermore, several multi-responsive BODIPY dyes, i.e., viscometers and pH-sensors, have been prepared.

In addition, a first successful liquid-solid extraction protocol for purification of a BODIPY dyes was developed. If proven to generally apply to BODIPY dyes, this approach should significantly facilitate and streamline the synthesis of BODIPY dyes, which would further enhance and expand the range of applications of these dyes.

5. ACKNOWLEDGEMENTS

This research was financially supported by TCU-SERC (SERC-UG 170318), TCU–Department of Chemistry & Biochemistry, and National Institutes of Health (NIH: 1R15GM135900-01). Special thanks go to: a) Guillaume Douady who directed on and assisted in the synthesis of various BODIPY dyes, b) Professor Gryczynski and his group (TCU-Physics and Astronomy) for photophysical studies on BODIPY dyes, and c) Professor Grygorczyk and his group (University of Montreal) for evaluation of cell permeability of BODIPY dyes.

I would also like to thank Sergei Dzyuba and the members of his group for providing guidance, advice, support and thought provoking conversations throughout my research at TCU.

6. REFERENCES

1. a) Loudet, A.; Burgess, K. BODIPY dyes and their derivatives: Synthesis and spectroscopic properties. *Chem. Rev.*, **2007**, *107*, 4891–4932; b) Ulrich, G.; Ziessel, R.; Harriman, A. The chemistry of fluorescent Bodipy dyes: versatility unsurpassed. *Angew. Chem. Int. Ed.,* **2008**, *47*, 1184–1201.
2. a) M. K. Kuimova, Mapping viscosity in cells using molecular rotors. *Phys. Chem. Chem. Phys.,* **2012**, *14*, 12671–12686; b) Klymchenko, A. S. Solvatochromic and fluoregenic dyes as environment-sensitive probes: Design and biological applications. *Acc. Chem. Res.,* **2017**, *50*, 366–375.
3. a) Uzhinov, B. M.; Ivanov, V. L.; Melnikov, M. Ya. Molecular rotors as luminescence sensors of local viscosity and viscous flow in solutions and organized systems. *Russ. Chem. Rev.*, **2011**, *80*, 1179–1190; b) Doan, H.; Raut, S. L.; Yale, D.; Balaz, M.; Dzyuba, S. V.; Gryczynski, Z. Mechanothermally induced conformational switch of a porphyrin dimer in a polymer film. *Chem. Commun.* **2016**, *52*, 9510–9513; c) Vysniaiskas, A.; Balaz, M.; Anderson, H. L.; Kuimova, M. K. Dual mode quantitative imaging of microscopic

viscosity using a conjugated porphyrin dimer. *Phys. Chem. Chem. Phys.*, **2015**, *17*, 7548–7554.

4. Sarder, P.; Maji, D.; Achilefu, S. Molecular probes for fluorescence lifetime imaging. *Bioconjugate Chem*., **2015**, *26*, 963–974.
5. a) Raut, S.; Kimball, J. D.; Fudala, R.; Bora, I.; Chib, R.; Jaafari, H.; Castillo, M. K.; Smith, N. W.; Dzyuba, S. V.; Gryczynski, Z. Triazine-based BODIPY trimer as a molecular viscometer. *Phys. Chem. Chem. Phys.,* **2016**, *18*, 4535–4530; b) Kimball, J. D.; Raut, S.; Jameson, L. P.; Smith, N. W.; Gryczynski, Z.; Dzyuba, S. V. BODIPY-BODIPY dyad: assessing the potential as a viscometer for molecular and ionic liquids. *RSC Adv.,* **2015**, *5*, 19508–19511; c) Raut, S.; Kimball, J.; Fudala, R.; Doan, H.; Maliwal, B.; Sabnis, N.; Lacko, A.; Gryczynksi, I.; Dzyuba, S. V.; Gryczynski, Z. A homodimeric BODIPY rotor as a fluorescent viscosity sensor for membrane-mimicking and cellular environments. *Phys. Chem. Chem. Phys.,* **2014**, *16*, 27037–27042.
6. Jameson, L. P.; Dzyuba, S. V. Facile, mechanochemical synthesis of BODIPY dyes. *Beilstein J. Org. Chem.,* **2013**, *9*, 786–790.
7. a) Elborn, J. S. Cystic fibrosis. *Lancet* **2016**, *388*, 2519–2531; b) Ehre, C.; Ridley, C.; Thornton, D. J. Cystic fibrosis: an inherited disease affecting mucin-producing organs. *Int. J. Biochem. Cell Biol.* **2014**, *52*, 136–145; c) Withers, A. L. Management issues for adolescents with cystic fibrosis. *Pulm Med*. **2012**, 134132.
8. a) Lai, S.K.; Wang, Y.Y.; Wirtz, D.; Hanes J. Micro- and macrorheology of mucus. *Adv. Drug Deliv. Rev*. **2009**, *61,* 86–100; b) Davies, J.C.; Alton, E.W.; Bush, A. Cystic fibrosis. *BMJ*, **2007**, *335*, 1255–1259.

9. Requena, S.; Ponomarchuk, O.; Castillo, M.; Rebik, J.; Brochiero, E.; Borejdo, J.; Gryczynski, I.; Dzyuba, S. V.; Gryczynki, Z.; Grygorczyk, R.; Fudala, R. Imaging viscosity of intragranular mucin matrix in cystic fibrosis cell. *Sci. Rep*., **2017**, 7, 16761.

10. a) Vanori, S.; Scantamburlo, G.; Dossena, S.; Paulmichi, M.; Nofziger, C. Interleukin-mediated Pendrin transcriptional regulation in airway and Esophageal Epithelia. *Int. J. Mol. Sci.*, **2019**, *20*, 731; b) Ambort, D.; Johansson, M. E. V.; Gustafsson, J. K.; Ermund, A.; Hansson, G. C. Perspectives on mucus properties and formation-lessons from the biochemical world. *Cold Spring Harbor Perspectives in Medicine,* **2012**, *2*, a014159/1-a014159/9.